Available online at www.sciencedirect.com
ScienceDirect
ELSEVIER
Palaeogeography, Palaeoclimatology, Palaeoecology 243 (2007) 174–188
PALAEO
www.elsevier.com/locate/palaeo

Estimating Pliocene sea-surface temperatures in the Mediterranean: An approach based on the modern analogs technique

Francisco Serrano *, José M. González-Donoso, Paul Palmqvist, Antonio Guerra-Merchán, Dolores Linares, Juan A. Pérez-Claros

Departamento de Ecología y Geología, Universidad de Málaga. Campus de Teatinos s/n, E-29071-Málaga, Spain

Received 7 April 2006; received in revised form 10 July 2006; accepted 14 July 2006

Abstract

The possibilities of adapting the Modern Analogs Technique (MAT) based on planktonic foraminifers for estimating sea-surface temperatures (SST) in the Mediterranean during the Pliocene are discussed in this article. The calibration database used comprises 684 core-top samples distributed in the North Atlantic and the Mediterranean. MAT estimates show an imperceptible bias (−0.03 °C; σ=0.59) and a low mean error of estimates (0.42 °C; σ=0.42) when applied over the samples of the calibration dataset. The procedure used for assimilating the Pliocene taxonomic categories to those of the modern assemblages results in an increase from 17 to 40 in the number of samples showing an error >2 °C when applied over the calibration database. However, the precision of MAT does not diminish when these samples are removed from the dataset. This methodology was used for obtaining SST estimates of late-middle Pliocene–earliest Pleistocene samples from ODP-site 975 (Menorca area), which have close modern analogs within the calibration database. In order to compare this technique with an additional proxy, we measured also $\delta^{18}O$ values of *G. bulloides* tests from these samples. The results obtained show a good agreement on the whole, which corroborates the validity of the technical approach proposed.

Keywords: Sea-surface temperature (SST); Modern Analogs Technique (MAT); Planktonic foraminifera; Pliocene; Mediterranean; $\delta^{18}O$

1. Introduction

If we assume that the ecological requirements of planktonic foraminiferal species do not change significantly through time, the composition of their assemblages may be used for inferring past environmental features as a function of their current requirements. This hypothesis has been mainly applied to estimating sea-surface temperatures (SST) during the Quaternary, which is achieved by comparing the taxonomic composition of the planktonic foraminiferal assemblages from Pleistocene and Holocene sediments with the ones accumulated in present days on the sea floor and the current surface temperatures for these areas.

Different techniques have been used for estimating SST values. Imbrie and Kipp (1971) developed a transfer function (TF) using *Q*-mode factor analysis and multiple regression in a set of core-top samples (for details on the methodology, see Klovan and Imbrie, 1971). This technique has been applied later by many authors (e.g., Imbrie et al., 1973; Kipp, 1976; Gardner and Hays, 1976; Molina-Cruz and Thiede, 1978; Thunell, 1979a; Hutson and Prell, 1980; Pujol, 1980; Molfino et al., 1982;

* Corresponding author. Fax: +34 952137386.
E-mail address: F.Serrano@uma.es (F. Serrano).

0031-0182/$ - see front matter © 2006 Elsevier B.V. All rights reserved.
doi:10.1016/j.palaeo.2006.07.012

Dowsett and Poore, 1990; Dowsett, 1991), whether as it was originally described by Imbrie and Kipp (1971) or following other mathematical approaches: multiple regression using as predictor variables the relative frequencies of species instead of the scores of faunal assemblages derived from factor analysis (Hutson, 1977); linear regression adjusted with the means of the optimum values of the environmental variables for each species, weighted according to their relative abundances (Berger and Gardner, 1975; Birks et al., 1990).

The Modern Analogs Technique (MAT; Hutson, 1980) represents an alternative to transfer functions based on the analysis of the faunal similarity between the fossil assemblages and the samples of a modern calibration dataset. González Donoso et al. (2000) used a variant of this methodology for obtaining sequences of palaeotemperatures during the Quaternary in the western Mediterranean. Although several authors (e.g., Hutson, 1977; Prell, 1985; Le, 1992; Pflaumann et al., 1996; Dowsett and Robinson, 1997; González-Donoso and Linares, 1998) have evaluated the different techniques proposed with the aim of determining the reliability of their results, no unanimously accepted conclusion has been reached.

The application of these methodologies for obtaining SST estimates for epochs older than the Pleistocene represents an unavoidable limitation, because the taxonomic composition of planktonic foraminiferal assemblages has changed through time. Several authors, however, have used variants of the techniques mentioned above for estimating SST values or for obtaining thermal indexes that reflect the climatic variations during the Neogene (Thunell, 1979a; Thunell, 1979b; Vergnaud-Grazzini, 1985; Zachariasse et al., 1989; Dowsett and Poore, 1990; Lourens et al., 1992; Dowsett et al., 1996; González Donoso et al., 1999; Serrano et al., 1999). The results obtained may depend to a great extent on the taxonomic treatment given to the non-common species and morphotypes. Thunell (1979a), Dowsett and Poore (1990), Dowsett (1991) and Dowsett and Robinson (1997) have proposed various ways for regrouping the taxonomic categories.

In this article we evaluate a modality of MAT specifically designed for obtaining SST estimates in the Pliocene of the Mediterranean, although it could also be applied to the whole North Atlantic. We assume several considerations for comparing Pliocene and Recent taxonomic categories, evaluating also the precision of the technique at each step. Using core samples of Pliocene sediments from ODP-site 975 (south of Menorca: 38° 53.8′ N, 43° 0.6′ E; Comas et al., 1996), we have tested if these Pliocene assemblages have close "modern analogs" within the calibration dataset. As an additional proxy, we have also compared the results of $\delta^{18}O$ analyses with the SST estimates obtained with MAT.

2. Methodology

González-Donoso and Linares (1998) evaluated more than 300 modalities of TF and MAT for estimating SST values and agreed with Dowsett and Robinson (1997) in considering that the best results are obtained with MAT using the squared chord distance (SCD) as a measure of dissimilarity. Using this coefficient, we have selected for each core sample analyzed the ten closest core-top samples of the calibration database (i.e., those that show less dissimilarity) and then we have calculated the mean SST value, weighting inversely the modern analogs selected as a function of their dissimilarity to the core sample. For each core sample, SST estimates for winter and summer were calculated as the mean temperature of the three colder and warmer months, respectively. The SST values presented in this article are mean annual temperatures, calculated as the arithmetic mean of summer and winter sea-surface temperatures. The degree of seasonality was calculated as the difference between summer-SST and winter-SST estimates.

2.1. The calibration dataset

The calibration dataset comprises 684 core-top samples distributed across the North Atlantic Ocean (N=515) and the Mediterranean Sea (N=169) (Fig. 1), using data from Gardner and Hays (1976), Kellogg (1976), Kipp (1976), Balsam and Flessa (1978) and Pujol (1980), as well as core-top data used by Thunnel (1978), Brunner (1979) and Loubere (1981) that were kindly provided to us by these authors. In addition, we complemented the dataset with other samples of the CLIMAP database (1984). In this way, the geographic coverage of our calibration dataset comprises semiconfined oceanographic realms such as the Mediterranean or the Gulf of Mexico that are poorly represented in the CLIMAP database.

On the contrary, the samples placed near the east coast of North America were removed from our database, because these core-tops did not show a good agreement between the assemblages of planktonic foraminifers and the SST values for these localities. This is probably related to the confluence of the cold waters of the Labrador stream with the warm waters of the Gulf stream, which results in a high and unstable thermal gradient in the surface waters of this region.

The quantitative composition of the assemblages from the core-tops of the calibration database comprises the

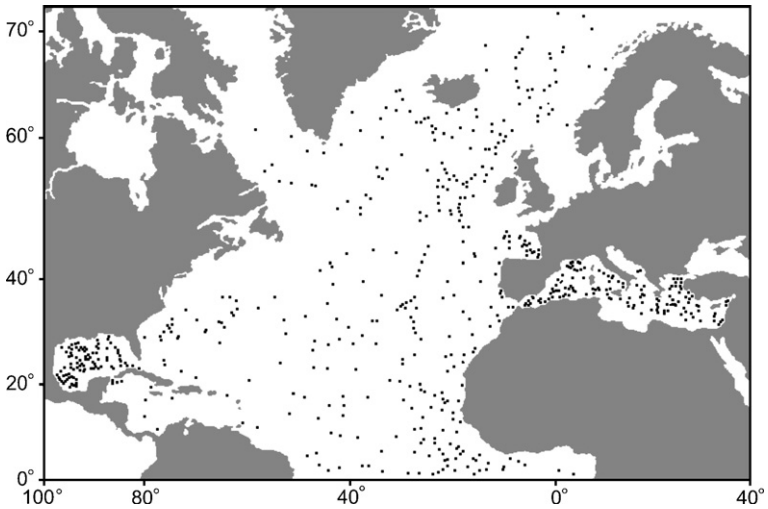

Fig. 1. Location of the core-tops of the calibration dataset used in this study.

relative abundance of 26 taxonomic categories of planktonic foraminifers (Table 1). The SST values associated to each sample were obtained from the archives of the National Oceanographic Data Center (NODC; Conkright et al., 2002).

2.2. Equivalence between the taxonomic categories of Pliocene and Recent assemblages

Before applying a MAT procedure, the same taxonomic categories must be represented in both the fossil samples analyzed and the calibration dataset. In order to get a correspondence between these categories (Table 1), we have made the following assumptions:

First, we assume that some taxonomic differences between the Pliocene and modern populations will represent the appearance or disappearance of morphotypes belonging to the same evolutionary species, and that these species have survived during the Plio-Quaternary. This implies that such species increased or reduced their morphological variability during this period of time. These cases are based on the frequent appearance of transitional forms during the interval of coexistence between the morphotypes, which in turn makes it difficult their taxonomic assignment. In some cases there are morphotypes that were differentiated by some authors in the Pliocene populations but not in the modern ones, or vice versa, although such morphotypes are actually present in both. Assuming this, we have grouped in the same taxonomic category the different morphotypes of each of these species; in doing so, we are also assigning to these groupings the environmental conditions in which the whole set of modern morphotypes of the species live today. Of course, there is always the possibility that some of these species may include what are in fact genetically different populations or even cryptic species, which may or may not have different oceanographic preferences (e.g., see Kucera and Darling, 2002). However, there is no genetic information available for the calibration dataset and, obviously, for the Pliocene samples. In addition, such approach would be only useful if each genetic variant could be correlated with a recognizable morphology.

According to all the above assumptions, we have performed the following modifications:

1. *G. conglobatus*, *G. ruber*, *G. elongatus*, *G. obliquus* and *G. extremus* (formal designations in Table 1) were considered morphological variants of the same evolutionary species and, as such, were grouped within the same category. All these morphotypes coexist in the middle part of the Pliocene, showing high frequencies and presenting clear morphological transitions among them. Currently, *G. Conglobatus* lives in warm waters (Table 2), within the range of temperatures inhabited by *G. ruber* (in the living populations, *G. elongatus* is not usually distinguished from *G. ruber*) and there are many specimens showing intermediate morphologies. Molecular data also indicate a close phylogenetic relationship between *G. ruber* and *G. conglobatus* (de Vargas et al., 1997).
2. According to the criterion presented above, we have also joined under the same category the group that includes the morphotypes *G. rubescens*, *G. tenellus*, *G. apertura*, *G. decoraperta* and *G. bulloideus*. Nowadays these forms do not reach high frequencies (they barely represent >0.1) and show less morphological variability than during the Pliocene, with *G. rubescens* occupying now a broader range of temperatures and *G. tenellus* being limited to the fringe of warmest waters

Table 1
Equivalence between the taxonomic categories identified in the Pliocene assemblages and in the core-tops of the calibration dataset

Calibration dataset	Pliocene
G. bulloides	***G. bulloides***
Globigerina bulloides d'Orbigny	*Globigerina bulloides* d'Orbigny
	Globigerina riveroae Bolli & Bermúdez
G. calida	***G. calida***
Globigerina calida Parker	*Globigerina calida* Parker
G. falconensis	***G. falconensis***
Globigerina falconensis Blow	*Globigerina falconensis* Blow
G. digitata	***G. digitata***
Globigerina digitata Brady	*Globigerina digitata* Brady
	Globigerina praedigitata Parker
***G. rubescens* group**	***G. rubescens* group**
Globigerina rubescens Hofker	*Globigerina rubescens* Hofker
Globigerinoides tenellus Parker	*Globigerina apertura* Cushman
	Globigerina decoraperta Takayanagi & Saito
	Globigerinoides tenellus Parker
	Globigerinoides bulloideus Crescenti
***G. ruber* group**	***G. ruber* group**
Globigerinoides conglobatus (Brady)	*Globigerinoides conglobatus* (Brady)
Globigerinoides ruber (d'Orbigny)	*Globigerinoides elongatus* (d'Orbigny)
	Globigerinoides extremus Bolli & Bermúdez
	Globigerinoides obliquus Bolli
	Globigerinoides ruber (d'Orbigny)
***G. trilobus* group**	***G. trilobus* group**
Globigerinoides sacculifer (Brady) without sacklike chamber	*Globigerinoides trilobus* (Reuss)
Globigerinoides sacculifer (Brady) with sacklike chamber	*Globigerinoides sacculifer* (Brady)
Neogloboquadrina	***Neogloboquadrina***
Neogloboquadrina dutertrei (d'Orbigny)	*Neogloboquadrina acostaensis* (Blow)
Neogloboquadrina pachyderma (Ehrenberg) dextral coiling	*Neogloboquadrina dutertrei* (d'Orbigny)
Neogloboquadrina pachyderma (Ehrenberg) sinistral coiling	*Neogloboquadrina humerosa* (Takayanagi & Saito)
	Neogloboquadrina pachyderma (Ehrenberg)
G. scitula	***G. scitula***
Globorotalia scitula (Brady)	*Globorotalia scitula* (Brady)
***G. inflata* group**	***G. inflata* group**
Globorotalia inflata (d'Orbigny)	*Globorotalia bononiensis* Dondi
	Globorotalia inflata (d'Orbigny)
	Globorotalia puncticulata (Deshayes)
***G. crassaformis* group**	***G. crassaformis* group**
Globorotalia crassaformis Galloway & Wissler	*Globorotalia aemiliana* Colalongo & Sartoni
	Globorotalia crassaformis Galloway & Wissler
***G. menardii* group**	***G. menardii* group**
Globorotalia cultrata (d'Orbigny)	*Globorotalia cultrata* (d'Orbigny)
Globorotalia menardii (Parker, Jones & Brady)	*Globorotalia menardii* (Parker, Jones & Brady)
Globorotalia tumida (Brady)	*Globorotalia plesiotumida* Blow & Banner
	Globorotalia tumida (Brady)
G. hirsuta	***G. hirsuta***
Globorotalia hirsuta (d'Orbigny)	*Globorotalia hirsuta* (d'Orbigny)
G. truncatulinoides	***G. truncatulinoides***
Globorotalia truncatulinoides (d'Orbigny) dextral coiling	*Globorotalia truncatulinoides* (d'Orbigny) dextral coiling
Globorotalia truncatulinoides (d'Orbigny) sinistral coiling	*Globorotalia truncatulinoides* (d'Orbigny) sinistral coiling
Globigerinella	***Globigerinella***
Globigerinella siphonifera (d'Orbigny)	*Globigerinella obesa* (Bolli)
	Globigerinella siphonifera (d'Orbigny)
Globigerinita	***Globigerinita***
Globigerinita glutinata (Egger)	*Globigerinita glutinata* (Egger)
Pulleniatina	***Pulleniatina***

(continued on next page)

Table 1 (*continued*)

Calibration dataset	Pliocene
Pulleniatina obliquiloculata (Parker & Jones)	*Pulleniatina obliquiloculata* (Parker & Jones)
Sphaeroidinella	***Sphaeroidinella***
Sphaeroidinella dehiscens (Parker & Jones)	*Sphaeroidinella dehiscens* (Parker & Jones)
	Sphaeroidinellopsis seminulina (Schwager)
Turborotalita	***Turborotalita***
Turborotalita quinqueloba (Natland)	*Turborotalita quinqueloba* (Natland)
Orbulina	***Orbulina***
Orbulina universa d'Orbigny	*Orbulina bilobata* d'Orbigny
	Orbulina suturalis Brönnimann

(Table 2). However, it is worth noting that both morphotypes show their highest frequencies in warm waters. In addition, it is usually difficult to distinguish if there are dorsal apertures in the specimens of this group or if such apertures are absent, even more in the Pliocene sediments, in which there is not always an optimal preservation.

3. As in Dowsett and Poore (1999), we have joined the keeled globorotaliids of the *G. cultrata* (including *G. menardii*) and *G. tumida* groups in a single category. Both groups are characteristic of warm waters (Table 2) and many specimens are difficult to assign unequivocally to one of them. In addition, when these forms are present in the samples they usually show very low relative frequencies. By this reason, their contribution for estimating palaeotemperatures using MAT is low.
4. *Neogloboquadrina* represents a particular case. Among modern populations, *N. dutertrei*, *N. pachyderma* dextral coiling and *N. pachyderma* sinistral coiling are usually distinguished, because each of these morphotypes has distinct oceanographic requirements (Table 2). However, the forms showing intermediate features between *N. dutertrei* and *N. pachyderma* are very frequent (in fact, they may represent the majority of the specimens in many samples) and there is evidence of gene flow between the populations of *Neogloboquadrina* (Darling et al., 2000, 2004). Also, we have increasing evidence that the relationship between temperature and coiling types may have changed during the upper Neogene. For example, the sediments from some stratigraphic intervals of late Miocene age in the Betic Cordillera, Southeastern Spain, show predominantly left coiling populations of *Neogloboquadrina* coexisting with high frequencies of specimens from species typical of warm waters, such as *G. extremus* and *G. trilobus*. Given these reasons, we choose to unify all the types of *Neogloboquadrina* under a single category.

A second group of modifications has been performed on the basis of several biostratigraphic events that take place during the Pliocene:

5. Given that *G. truncatulinoides* appears by the end of the Pliocene, we have removed this taxonomic category. In this way, we have applied jointly all the modifications detailed above (i.e., modifications 1–5) for estimating SST values during the middle-late Pliocene, which implicitly means that the calibration database is reduced from 26 to 19 taxonomic variables (originally, it included *G. truncatulinoides* dextral and sinistral coiling as different variables).
6. Taking into account that the group of *G. crassaformis* appears by the beginning of the middle Pliocene, we have not considered this taxonomic category for evaluating SST changes during the early Pliocene (Zanclean).
7. *Globorotalia hirsuta* and *Globorotalia margaritae* are two similar forms that show unresolved taxonomic, phylogenetic and biostratigraphic aspects (for review, see Kennett and Srinivasan, 1983; Bolli and Saunders,

Table 2
Representative temperatures deduced from the calibration data set for those taxa and categories involved in the modifications

Taxa and taxonomic categories	Maximum frequency	Max. frequency SST (°C)	SST (°C) range	Weighted average SST (°C)
G. conglobatus	0.1	26.7	20.3–27.6	25.0
G. ruber	0.817	25.7	10.8–27.8	23.3
***G. ruber* group**	0.827	25.7	10.8–27.8	23.4
G. rubescens	0.145	27.1	10.4–27.6	22.3
G. tenellus	0.114	26.4	17.9–27.3	23.5
***G. rubescens* group**	0.175	26.4	10.4–27.8	22.8
G. menardii	0.309	24.4	18.4–27.8	25.9
G. tumida	0.84	26.2	22.2–27.6	26.6
***G. menardii* group**	0.847	26.2	18.3–27.8	26.2
G. dutertrei	0.32	27.2	8.3–27.8	25.2
G. pachyderma dex.	0.8	8.8	2.6–27.5	14.1
G. pachyderma sin.	0.98	4.2	2.6–24.7	7.3
Neogloboquadrina	0.997	4.2	2.6–27.8	13.7
***G. inflata* group**	0.54	18.4	6.9–27.8	18.5

SST ranges only for frequencies >0.01. Weighted average temperatures calculated as a function of the frequencies of taxa.

1985; Iaccarino, 1985). By this reason, in order to derive SST estimates for the Zanclean we discarded *G. hirsuta* from the calibration dataset and we did not take into account the specimens of *G. margaritae* from the Pliocene samples. Therefore, the SST estimates for the late Zanclean were estimated using the combination of all the modifications presented before (i.e., modifications 1–7)

8. The last action affects *Globorotalia inflata*, which is a major component of the modern assemblages from temperate waters (Table 2). Apart from *G. inflata*, during the Pliocene there are two forms that are morphologically similar, *G. puncticulata* and *G. bononiensis*. The prevalence of each of the three forms changes through the Pliocene, but the transitional morphologies between them are common, which points to their close phylogenetic relationship. In the light of the species with which they use to be associated, the high frequency of this group during the Pliocene seems to be also in relation to the establishment of temperate regimes (Zachariasse et al., 1989). As a consequence, we have assigned the environmental requirements deduced for the living populations of *G. inflata* to this group of morphotypes. In addition, we have combined all the modifications discussed above and the suppression of *G. inflata* from the calibration database (modifications 1 to 8) for estimating the SST values of the samples placed before the appearance of *G. puncticulata* (early Zanclean).

In agreement with the actions detailed above, the calibration dataset used for estimating SST during the Pliocene has between 19 and 16 categories, depending on the Pliocene interval analyzed. Obviously, this forced us to recalculate the relative frequencies of the categories considered in each case.

3. Results and discussion

The methodology proposed has been tested using two different approaches:

Firstly, we have analyzed the precision of the technique when applied over the universe of modern core-top samples. In doing so, in a preliminary test we extracted

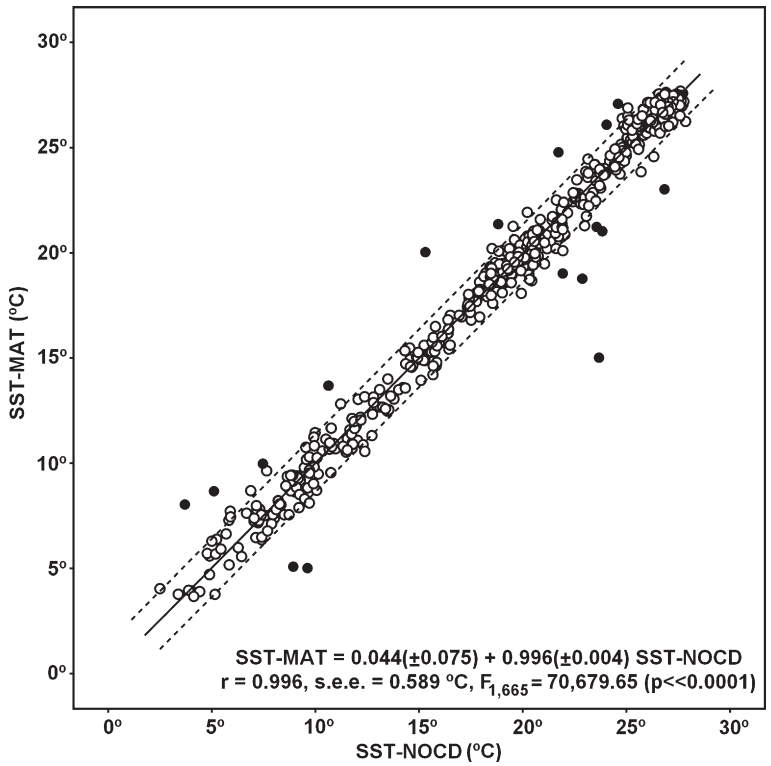

Fig. 2. SST estimates derived using MAT vs. SST values obtained from the NOCD database. The equation of the least-squares regression line and the value of the correlation coefficient are shown. Filled circles indicate the 17 outliers removed from the dataset before the adjustment. Dashed lines show the $p<0.01$ confidence interval above and below the regression line. The standard errors of the *Y*-intercept and the slope are shown between bracketts; *r*: Pearson product-moment correlation coefficient; s.e.e.: standard error of the estimate; $F_{1,665}$: *F*-test of overall fit with 1 and 665 degrees of freedom.

each sample from the calibration database (i.e., the leave-one-out method) and compared the SST estimates obtained from MAT with the SST values of the NOCD database. After this, we analyzed the changes in precision that result from the application of the taxonomic modifications performed for adapting the universe of calibration to the Pliocene assemblages.

Secondly, we have obtained the SST estimates of a set of Pliocene and earliest Pleistocene core samples from ODP-site 975 (Comas et al., 1996) using MAT. In order to estimate the reliability of the results, we have tested if these samples have close modern analogs in the calibration dataset before deriving their SST values. As an additional test, we have compared the measurements of $\delta^{18}O$ in *G. bulloides* specimens from these Pliocene samples with the SST estimates.

3.1. Testing MAT on the calibration dataset

Two statistic parameters were calculated for evaluating the error of the SST estimates obtained using MAT: (1) the mean error of SST estimates, calculated as the average difference between the temperatures predicted with this technique and those expected from the NOCD database; and (2) the mean absolute error of SST estimates, calculated using the absolute value of the differences between the SST estimates and the NOCD temperatures. The first approach measures the bias of the estimates, which allows detecting if the SST estimates obtained with MAT show a significant, non-random deviation from the SST values of the NOCD database. If the mean difference is close to zero, this means that there is no systematic overestimation or underestimation of SST values, and thus no significant bias. However, this approach does not measure the accuracy of the methodology for providing precise SST estimates (i.e., the overall difference between the expected and predicted values). This is measured by the mean absolute error of the estimates.

The comparison of the SST estimates derived from MAT with the temperatures of the NOCD database for the 684 core-top samples of the calibration dataset shows a high concordance. The correlation between SST–MAT and SST–NOCD values is very high ($r=0.991$, $p<<0.001$) and deviations >2 °C occur in only 17 samples (2.49% of cases). In fact, there is a low scatter of the samples around the regression line adjusted by the least-squares method after the removal of these outliers (Fig. 2). In addition, the values of both the *Y*-intercept (0.044) and the slope (0.996) are close to those expected (i.e., 0 and 1, respectively) from a strict correspondence between SST–MAT and SST–NOCD. Given its standard error (0.075), the value adjusted for the *Y*-intercept does not differ significantly from the expected one according to a *t*-test ($t=0.59$, two-tailed; $p>>0.1$). This indicates that there is no systematic bias towards higher or lower SST estimates. On the other hand, the value adjusted for the slope, given its standard error (0.004), is not significantly different from the one expected according to a *t*-test ($t=1.01$, two-tailed; $p>>0.1$). This implies that MAT does not overestimate the high temperatures and underestimate the low ones or vice versa. In other words, the errors in the SST estimates are randomly distributed.

In order to enhance even more the precision of MAT and in accordance with the results exposed in the above paragraph, we have made all the calculations extracting from the calibration database those samples with an error >2 °C for SST estimates. The results obtained (Table 3) show that the deviation from zero of the mean difference between SST–MAT and SST–NOCD values is minimal (bias = −0.03 °C; $\sigma=0.59$). This indicates again that, on average, MAT does not overestimate or underestimate the temperatures (Table 3). In addition, the absolute values of the differences between SST–MAT and SST–NOCD show that the mean error estimate for MAT is of only 0.42 °C ($\sigma=0.42$).

Following the same procedure, we have calculated also the changes in the precision of MAT estimates derived from the modifications proposed for the taxonomic categories as well as the accumulative loss derived from the modifications that were applied jointly to each different Pliocene interval (Table 3).

Firstly, the unification of the forms of *G.* gr. *ruber* (modification 1), *G.* gr. *rubescens* (modification 2) and

Table 3
Evaluation of the precision of MAT estimates on the samples of the calibration data set for each modification applied separately and also for the combinations of modifications used for estimating Pliocene SST values

Modifications	Calibration dataset (samples/variables)	Absolute error >2 °C	Bias±σ (°C)	Average error ±σ (°C)
Non-Mod.	667/26	17 (2.49%)	0.03±0.59	0.42±0.42
1	667/25	17 (2.49%)	0.03±0.59	0.42±0.42
2	666/25	18 (2.63%)	0.03±0.59	0.42±0.42
3	667/25	17 (2.49%)	0.03±0.60	0.42±0.42
4	654/24	30 (4.39%)	0.03±0.58	0.40±0.41
5	663/24	21 (3.07%)	0.04±0.60	0.43±0.42
6	666/25	18 (2.63%)	0.04±0.59	0.42±0.41
7	663/25	21 (3.07%)	0.03±0.58	0.41±0.41
8	668/25	16 (2.34%)	0.02±0.60	0.42±0.42
1–4	657/21	27 (3.95%)	0.03±0.58	0.41±0.41
1–5	651/19	33 (4.82%)	0.02±0.59	0.42±0.42
1–7	647/17	37 (5.41%)	0.02±0.59	0.41±0.42
1–8	644/16	40 (5.84%)	0.02±0.58	0.41±0.41

G. gr. *menardii* (modification 3) does not result in a substantial loss of precision compared to the results obtained using 26 categories in the calibration dataset. In these cases, there are 17–18 samples that show an error >2 °C and both the errors and the standard deviations remain nearly unchanged.

Secondly, to group all the forms of *Neogloboquadrina* in a single variable (modification 4) results in no loss of precision for MAT, because both the bias (−0.03 °C; σ=0.58) and the mean error of estimates (0.40 °C; σ=0.41) remain almost unchanged. The more noticeable feature is an increase to 30 samples showing an absolute error >2 °C. Although a loss of precision could be expected *a priori* because we have eliminated the thermal discrimination produced by the coiling types of *N. pachyderma* and the relative abundance of *N. dutertrei*, this loss is really negligible and, after all, the modification is convenient if it is finally confirmed that the relationship between temperature and coiling types has changed during the late Neogene. In addition, it is remarkable that the joint application of the four modifications indicated above implies a minor change in the number of samples with error >2 °C, 27 compared to 30 when all the forms of *Neogloboquadrina* are grouped in the same variable (modification 4).

Table 4
Relative frequencies of taxa in the planktonic foraminiferal assemblages of the ODP-site 975 core samples of middle-late Pliocene– earliest Pleistocene age

mcd	bull	cal	ruber	crass	sph	dig	neog	falc	gnita	hirs	infl	men	pull	tita	rubs	tril	scit	gnell	orb
108.2	0.126	0.002	0.162	0.000	0.000	0.000	0.425	0.007	0.048	0.000	0.150	0.000	0.000	0.000	0.004	0.000	0.000	0.017	0.057
109.2	0.252	0.003	0.106	0.000	0.000	0.000	0.308	0.029	0.042	0.000	0.183	0.000	0.000	0.034	0.016	0.003	0.011	0.008	0.005
110.2	0.270	0.014	0.356	0.000	0.000	0.000	0.101	0.047	0.061	0.000	0.007	0.000	0.000	0.007	0.011	0.000	0.000	0.054	0.072
111.2	0.191	0.002	0.011	0.000	0.000	0.000	0.450	0.017	0.019	0.000	0.222	0.000	0.000	0.021	0.007	0.000	0.042	0.005	0.012
112.2	0.124	0.000	0.091	0.000	0.000	0.000	0.228	0.016	0.055	0.000	0.309	0.000	0.000	0.013	0.029	0.000	0.000	0.059	0.065
113.2	0.124	0.006	0.264	0.000	0.000	0.000	0.134	0.022	0.041	0.000	0.185	0.000	0.000	0.000	0.038	0.153	0.000	0.013	0.019
114.2	0.134	0.006	0.191	0.002	0.000	0.000	0.165	0.008	0.274	0.000	0.167	0.000	0.000	0.010	0.022	0.006	0.002	0.008	0.004
115.3	0.083	0.011	0.061	0.000	0.000	0.000	0.524	0.014	0.018	0.000	0.249	0.000	0.000	0.004	0.007	0.000	0.007	0.004	0.018
116.5	0.084	0.000	0.105	0.007	0.000	0.000	0.434	0.014	0.052	0.000	0.227	0.000	0.000	0.010	0.007	0.000	0.014	0.031	0.014
117.5	0.173	0.005	0.238	0.000	0.000	0.000	0.332	0.011	0.063	0.000	0.085	0.000	0.000	0.014	0.024	0.011	0.005	0.005	0.033
118.5	0.083	0.000	0.259	0.000	0.000	0.000	0.226	0.006	0.027	0.000	0.289	0.000	0.000	0.006	0.003	0.000	0.003	0.018	0.080
119.5	0.100	0.000	0.326	0.000	0.000	0.000	0.151	0.016	0.057	0.000	0.299	0.000	0.000	0.003	0.006	0.005	0.003	0.008	0.027
120.5	0.073	0.000	0.227	0.004	0.000	0.000	0.350	0.011	0.064	0.000	0.233	0.000	0.000	0.004	0.008	0.006	0.000	0.015	0.004
121.5	0.117	0.003	0.252	0.003	0.000	0.000	0.285	0.003	0.078	0.000	0.177	0.000	0.000	0.006	0.027	0.003	0.000	0.015	0.030
122.5	0.122	0.003	0.349	0.000	0.000	0.000	0.321	0.014	0.035	0.000	0.057	0.000	0.000	0.008	0.016	0.005	0.000	0.019	0.051
123.5	0.047	0.011	0.192	0.000	0.000	0.000	0.446	0.006	0.078	0.000	0.134	0.000	0.000	0.011	0.014	0.000	0.003	0.011	0.047
124.5	0.148	0.000	0.301	0.000	0.000	0.000	0.243	0.003	0.101	0.000	0.106	0.000	0.000	0.011	0.023	0.014	0.000	0.006	0.045
125.4	0.267	0.039	0.055	0.000	0.000	0.000	0.399	0.013	0.029	0.000	0.128	0.000	0.000	0.055	0.000	0.000	0.000	0.000	0.016
126.0	0.122	0.003	0.054	0.000	0.000	0.000	0.457	0.012	0.057	0.000	0.224	0.000	0.000	0.045	0.003	0.006	0.000	0.009	0.009
128.3	0.096	0.000	0.128	0.000	0.000	0.000	0.279	0.010	0.096	0.000	0.276	0.000	0.000	0.016	0.019	0.000	0.000	0.029	0.051
129.3	0.117	0.005	0.243	0.000	0.000	0.000	0.294	0.005	0.100	0.000	0.157	0.000	0.000	0.012	0.016	0.005	0.002	0.028	0.016
130.4	0.153	0.003	0.237	0.000	0.000	0.000	0.294	0.003	0.097	0.000	0.110	0.000	0.000	0.013	0.013	0.003	0.000	0.023	0.050
131.3	0.101	0.000	0.098	0.008	0.000	0.000	0.344	0.010	0.095	0.000	0.273	0.000	0.000	0.020	0.006	0.008	0.003	0.025	0.010
132.3	0.084	0.000	0.029	0.000	0.003	0.000	0.468	0.008	0.045	0.000	0.271	0.000	0.000	0.050	0.008	0.003	0.000	0.008	0.024
133.4	0.052	0.003	0.359	0.000	0.000	0.000	0.263	0.000	0.043	0.000	0.182	0.000	0.000	0.000	0.037	0.006	0.000	0.009	0.046
134.3	0.129	0.000	0.138	0.000	0.000	0.000	0.186	0.012	0.038	0.000	0.450	0.000	0.000	0.000	0.012	0.003	0.003	0.009	0.021
143.8	0.077	0.000	0.370	0.003	0.000	0.000	0.139	0.005	0.081	0.000	0.049	0.000	0.000	0.000	0.052	0.126	0.000	0.015	0.082
144.8	0.618	0.000	0.007	0.000	0.000	0.000	0.209	0.059	0.037	0.000	0.000	0.000	0.000	0.004	0.018	0.000	0.000	0.015	0.033
151.2	0.376	0.000	0.075	0.004	0.000	0.000	0.168	0.057	0.079	0.000	0.018	0.000	0.000	0.000	0.090	0.000	0.000	0.054	0.079
184.2	0.110	0.003	0.183	0.000	0.000	0.000	0.243	0.010	0.093	0.000	0.000	0.000	0.000	0.000	0.066	0.169	0.003	0.043	0.076
185.2	0.144	0.000	0.266	0.000	0.000	0.000	0.316	0.022	0.043	0.005	0.002	0.000	0.000	0.000	0.079	0.031	0.000	0.062	0.029
186.2	0.146	0.000	0.174	0.158	0.000	0.000	0.179	0.012	0.060	0.005	0.000	0.000	0.000	0.000	0.043	0.119	0.000	0.048	0.057
187.2	0.175	0.000	0.324	0.003	0.000	0.000	0.156	0.019	0.051	0.000	0.003	0.000	0.000	0.000	0.081	0.070	0.000	0.054	0.065
187.7	0.159	0.000	0.339	0.000	0.000	0.000	0.153	0.018	0.094	0.000	0.000	0.000	0.000	0.000	0.083	0.068	0.003	0.041	0.041
188.7	0.222	0.000	0.117	0.088	0.000	0.000	0.193	0.029	0.096	0.012	0.038	0.000	0.000	0.000	0.126	0.012	0.000	0.009	0.058
189.2	0.206	0.000	0.215	0.174	0.000	0.000	0.084	0.009	0.081	0.006	0.025	0.000	0.000	0.000	0.059	0.075	0.000	0.040	0.025
190.2	0.181	0.000	0.229	0.000	0.000	0.000	0.138	0.017	0.057	0.000	0.000	0.000	0.000	0.000	0.069	0.244	0.000	0.037	0.029

mcd: meter composite depth; bull: *G. bulloides*; cal: *G. calida*; ruber: *G. ruber* group; crass: *G. crassaformis* group; sph: *Sphaeroidinella*; dig: *G. digitata*; neog: *Neogloboquadrina*; falc: *G. falconensis*; gnita: *G. glutinata*; hirs. *G. hirsuta*; infl: *G. inflata* group; men: *G. menardii* group; pull: *Pulleniatina*; tita: *T. quinqueloba*; rubs: *G. rubescens* group; tril: *G. trilobus* group; scit: *G. scitula*; gnell: *Globigerinella*; orb: *Orbulina*.

The modifications performed as a function of the Pliocene bioevents do not imply, when applied individually, a significant loss of precision for MAT. In all cases (modification 5: removal of *G. truncatulinoides*; modification 6: removal of *G. crassaformis*; modification 7: removal of *G. hirsuta*; and modification 8: removal of *G. inflata*) the estimates with an error >2 °C oscillate between 16–21 samples, and both the bias and the mean error remain nearly unchanged. It is worth noting that the removal from the calibration dataset of *G. inflata*, a morphotype very abundant in the middle latitudes, implicitly results in a slight increase of the precision of MAT, which affects the number of samples with error >2 °C (16 compared to 17).

If we pay attention to the combinations of modifications applied for obtaining SST estimates for the middle-late

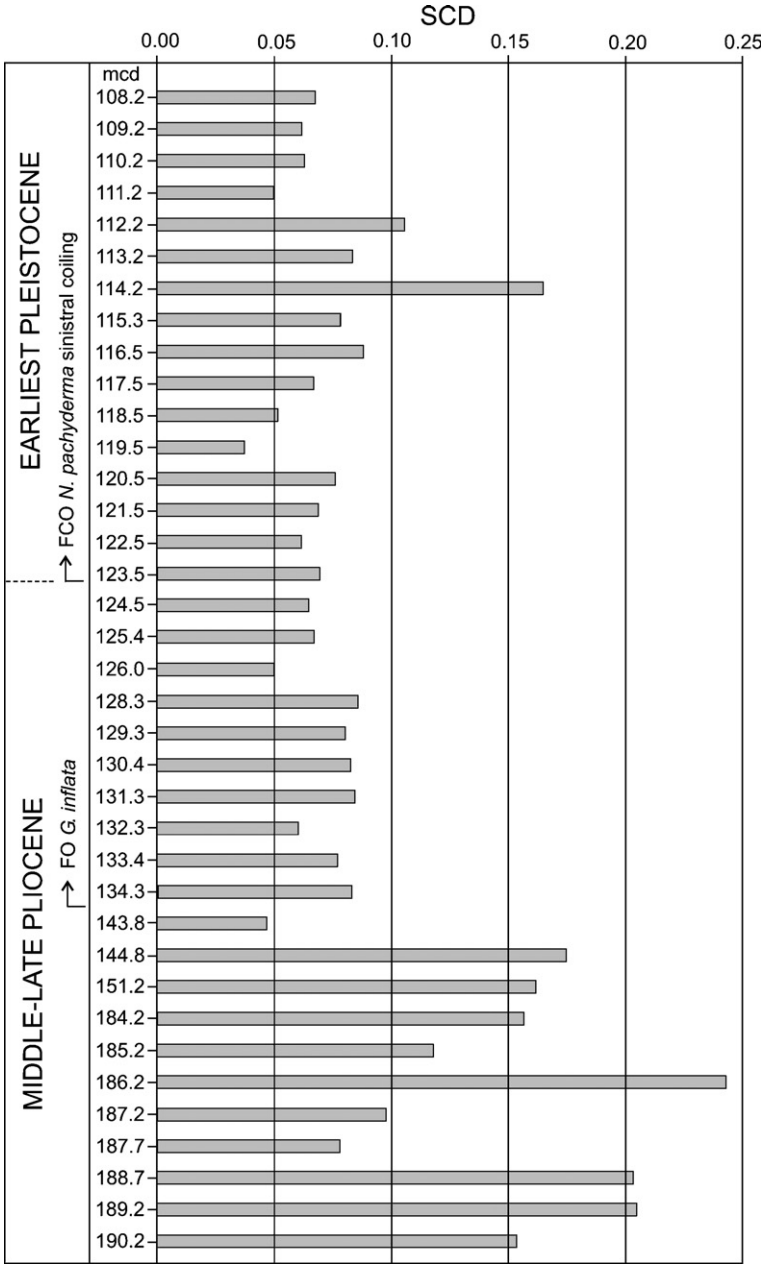

Fig. 3. Squared chord distance between the middle-late Pliocene – earliest Pleistocene ODP-site 975 core samples and their nearest modern analogs in the calibration dataset.

Pliocene (modifications 1 to 5 performed jointly; Table 3), there is no significant loss of precision in relation to the one derived from the removal of *Neogloboquadrina* (modification 4). In fact, there is only a minor increase in the number of samples showing an error >2 °C, which now comes to 33.

Similar results are obtained when the modifications 1–7 are applied simultaneously for obtaining SST estimates for the late Zanclean. After eliminating the 37 samples which show an error >2 °C, both the bias and the mean error remain nearly unchanged. The set of modifications

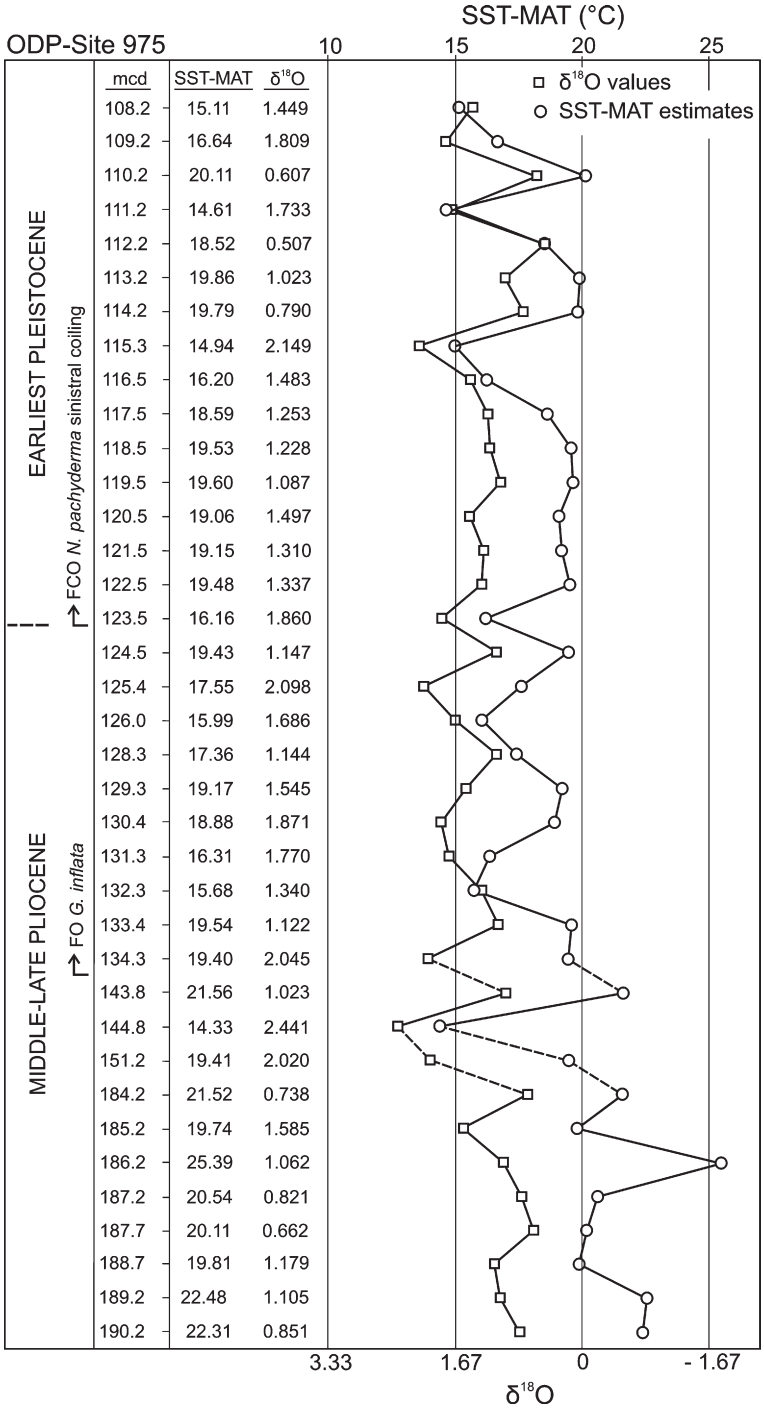

Fig. 4. Comparison between MAT-based SST estimates and $\delta^{18}O$ values for the ODP-site 975 core samples.

performed for estimating the SST values during the early Zanclean (modifications 1 to 8) increase the number of samples with error > 2 °C to 40, but the precision of MAT does not decrease when these samples are removed from the calibration database.

3.2. Test in Pliocene sediments: modern analogs and isotopic results

We used 37 samples from ODP-site 975 (Comas et al., 1996) located between 108.2 and 190.2 meters composite depth (mcd) for checking the proposed methodology. Although most of these samples are of middle-upper Pliocene sediments, we have also included several samples of the lowermost Pleistocene in order to record the cold interval that characterizes the Plio-Pleistocene transition. The composition of the assemblages of planktonic foraminifers was calculated using more than 300 specimens per sample from the > 160 μm fraction (relative frequencies of taxa in Table 4). It is worth noting that these samples show no evidence of faunal dissolution (e.g., microfossils scarce or predominantly broken).

As a previous step for determining if these fossil samples have close modern analogs, we have estimated the reciprocal of the squared chord distance (SCD) of each of the 37 samples with the core-tops of the calibration database. Considering that SCD values can range theoretically between 0 and 2, Dowsett and Robinson (1997) used an SCD value of 0.26 as a cutoff for analogous samples. In our case, given that for any fossil sample there is always a core-top sample in the calibration database that shows SCD < 0.25 (Fig. 3), we can consider that they all have modern analogs. In general terms, the samples placed above the first occurrence (FO) of *G. inflata* (135 mcd; Serrano et al., 1999) show SCD < 0.1, and those from the interval 143.8–190.2 mcd, where the specimens of the group of *G. inflata* are very scarce, have somewhat higher SCD values.

As an additional test for checking the SST estimates derived from MAT, we measured oxygen-isotopes ratios in tests of *G. bulloides* ($\delta^{18}O_{bull}$) from each of the 37 ODP-975 samples analyzed and compared the results with SST estimates calculated using modifications 1 to 5 jointly. In order to interpret the results of this comparison, we must assume that the $\delta^{18}O$ of the calcite of *G. bulloides* tests is controlled by the $\delta^{18}O$ of the surrounding water, which depends on the ice-sheet volume and also on the local salinity, and by the temperature of calcification (Maslin et al., 1995).

The $\delta^{18}O_{bull}$ values of the ODP-975 samples show a statistically significant, negative correlation with the SST estimates ($r = -0.609$; $p << 0.001$), which is reflected in noticeably parallel curves of $\delta^{18}O_{bull}$ and SST through time if the scale of the former is reversed (Fig. 4). The worst results are obtained in the interval between the samples 125.4 and 132.3 mcd, where the changes in $\delta^{18}O_{bull}$ ratios seem to precede those in SST values, with a lag of ~ 1 m of sediment (i.e., the average sampling interval). This would correspond to a time lag of 30 ka according to the average sedimentation rate estimated for this section of ODP-site 975 (Serrano et al., 1999), which seems too long to be caused by water mixing related to variations in the global ice-sheet volume. This suggests the absence of a cause and effect relationship for this apparent lag between the changes in SST and $\delta^{18}O_{bull}$ values. Another anomaly that should be emphasized is the SST peak (25.4 °C) of sample 186.2 mcd, which is not reflected in a remarkably low $\delta^{18}O_{bull}$ value, as could be expected. However, the taxonomic composition of this sample (Table 4) reflects high frequencies of species from warm waters (*G. crassaformis*, *G. ruber*, *G. trilobus*, *Globigerinella*, and *G. rubescens*). In fact, the closest modern analog of this sample is located in the equatorial area (9°55′ N, 20°58′ W), showing a SST of 26.25 °C and 3.28 °C of seasonality. All these anomalous values suggest that other factors (e.g., salinity changes related to changes in the regional hydrological balance, see below) must be significantly involved in determining the $\delta^{18}O_{bull}$ proportions.

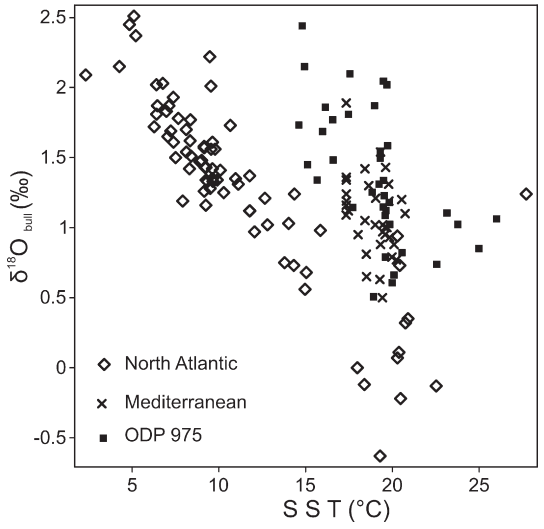

Fig. 5. SST vs. $\delta^{18}O$ ratios in North Atlantic and Mediterranean core-top samples as well as in the ODP-site 975 core samples. Core-top $\delta^{18}O$ ratios are from Duplessy et al. (1991) and Kallel et al. (1996). SST values for these core-tops are the averages between the mean temperatures of the three warmer and three colder months, obtained from NOCD database (Conkright et al., 2002).

A comparison of these results with available data of $\delta^{18}O$ ratios of *G. bulloides* tests (Duplessy et al., 1991; Kallel et al., 1996) from 109 North Atlantic and Mediterranean core-tops is shown in Fig. 5. It is worth mentioning that the North Atlantic core-tops show an inverse relationship between SST and $\delta^{18}O_{bull}$ ($r=-0.84$, $p<<0.001$, $N=75$), which is slightly more significant than the one obtained for the ODP-975 samples. However, such relationship is not evident in the case of the Mediterranean samples ($r=-0.28$, $p>0.05$, $N=34$), which show higher $\delta^{18}O_{bull}$ proportions (~ 1‰, on average) than those North Atlantic core-tops with similar SST values. Fig. 5 reveals that although many ODP-site 975 core samples plot over SST and $\delta^{18}O_{bull}$ values typical of the Mediterranean, there is a number that show combinations of SST estimates and $\delta^{18}O_{bull}$ ratios that do not match those of modern core-tops. Specifically, some of these ODP-975 samples with lower SST values than the ones recorded in the Mediterranean show also $\delta^{18}O_{bull}$ ratios higher than those North Atlantic core-tops with

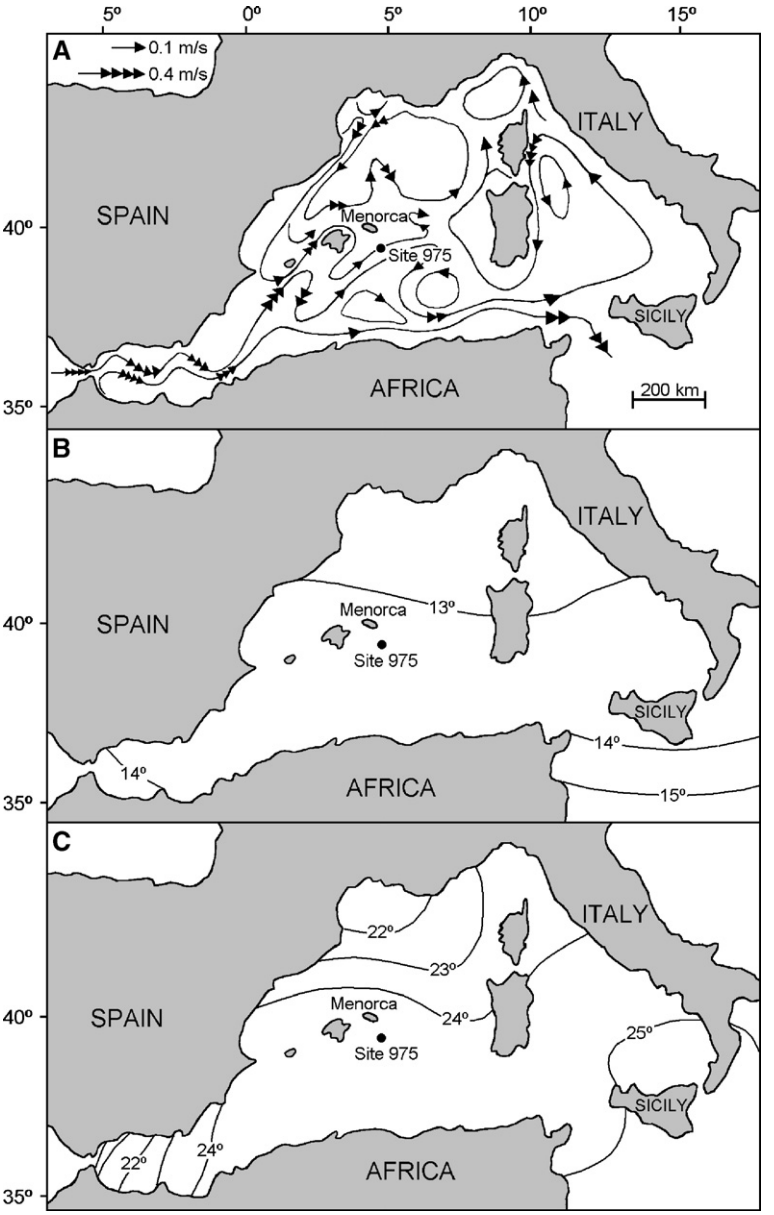

Fig. 6. Oceanographic features in the western Mediterranean. A: Sea-surface circulation patterns (data from Hopkins, 1985). B–C: Sea-surface isotherms for February and August, respectively (data from Gorshkov, 1978).

similar SST values. Such non-analogue frame may represent increases of the $\delta^{18}O$ values of surface waters due to increases in the global ice-sheet volume resulting from the cooler conditions of the Plio-Pleistocene transition. In fact, only one of these samples (144.8 mcd) is placed below the first occurrence (FO) of *G. inflata*, while six are located from the first common occurrence (FCO) of *N. pachyderma* sinistral coiling (123,5 mcd) onwards. Given that no magnetostratigraphic data are available for ODP-975, this datum could be used for identifying the beginning of the Pleistocene (González Donoso et al., 2000). In addition, there are a few ODP-site 975 core samples placed below the FO of *G. inflata* that show the highest SST values and relatively low $\delta^{18}O_{bull}$ ratios. These samples represent warmer conditions than those recorded now in the Mediterranean.

In summary, our results show a good agreement between most $\delta^{18}O_{bull}$ values and our SST estimates for the middle-late Pliocene and the earliest Pleistocene of the Mediterranean, although there are also noticeable exceptions. These exceptions, however, are not unexpected in a restricted, semiconfined marginal sea such as the Mediterranean, whose negative hydrological balance translates in an anti-estuarine circulation pattern (i.e., input of surface waters and output of deeper waters).

In the Mediterranean, the changes of temperature are induced by the general climatic variations and also depend on the configuration of the circulation patterns. Present-day SST values in the Mediterranean are conditioned by the input of relatively cold Atlantic waters and by the inner circulation that results in important thermal differences. Specifically, the loss by evaporation in the Mediterranean exceeds the inputs from precipitation and fluvial sources. This hydrological deficit generates the entry of surface North Atlantic cold waters with lower salinities (and thus lower $\delta^{18}O$ values) than the more saline Mediterranean waters of the Eastern basin. In fact, the water volume entering the Mediterranean via the Strait of Gibraltar is about twenty times greater than the quantity required to compensate for this deficit (Bethoux, 1980). This results in a deeper water current moving in the opposite direction that removes water from the Mediterranean. The Alboran Sea is affected by the entry of these cool waters, but the main body of the surface current flows close to the African coastline due to the Coriolis effect, reaching the eastern basin through the Strait of Sicily (Fig. 6A). For this reason, the temperature of the waters in the Menorca area is less influenced by the Atlantic current. In winter, the northern part of the western Mediterranean is subject to cold, dry winds from the continent that evaporate and cool the waters, leading to an increase in density. As a result, there is a mixing and homogenization of the whole water column at temperatures of ~ 13 °C (Fig. 6B). In summer, however, the more superficial water is mainly of Atlantic origin, but heated by insolation up to ~ 24 °C (Fig. 6C). Below this layer, there are warmer, more saline waters coming from the eastern Mediterranean that tend to mix with the upper layer. These conditions explain the high seasonality in the Menorca area.

The changes in the ice-sheet volume may have not paralleled the thermal changes in the Mediterranean waters, particularly if such changes modified the hydrologic balance. From this point of view, we may consider that the results provided by the $\delta^{18}O_{bull}$ ratios of the ODP-975 samples and those derived from the SST estimates obtained using MAT are complementary, with the $\delta^{18}O_{bull}$ values reflecting mainly the general palaeoclimatic trends and the local variations of salinity, while MAT estimates provide a more detailed picture on the thermal evolution of this particular area.

4. Conclusions

MAT techniques may represent a useful tool for estimating SST values during the Pliocene, provided that an appropriate equivalence between the Pliocene and modern taxonomic categories is achieved.

When the precision of MAT is evaluated over the calibration database, the modifications of the taxonomic categories proposed for this comparison result in a slight decrease of accuracy, which specifically affects the number of samples with higher absolute errors of the estimates. In the less favorable case, the number of samples with an error >2 °C increases from 17 to 40 out of 684, which corresponds to the set of modifications proposed for estimating the SST values of the lower Zanclean (modifications 1 to 8). However, once all the samples showing an error >2 °C have been removed, the initial precision (bias = −0.03 °C, σ = 0.59; mean error = 0.42 °C, σ = 0.42) remains nearly unchanged in all the cases.

The comparison between the $\delta^{18}O$ values and the SST estimates obtained from MAT for the middle-late Pliocene and earliest Pleistocene samples of the western Mediterranean (ODP-site 975, Leg 161) shows a good agreement. This is especially remarkable if we take into account that they do not represent the same effects, as both salinity and ice volume changes may have played a role in determining the $\delta^{18}O_{bull}$ values. Therefore, both datasets may be used in a complimentary way for depicting the general palaeoclimatic trends and the particular evolution of this area, respectively.

Acknowledgments

This study was carried out as part of the research by Group RNM-146 of Junta de Andalucía and within projects REN2002-01059, BTE2001-4903, and CGL04-01615 of the Spanish Ministry of Science and Technology. We also acknowledge the insightful comments and constructive remarks provided by the editor and two anonymous reviewers.

References

Balsam, W.L., Flessa, K.W., 1978. Patterns of planktonic foraminiferal abundance and diversity in surface sediments of the western North Atlantic. Marine Micropaleontology 3, 279–294.

Berger, W.H., Gardner, J.V., 1975. On the determination of Pleistocene temperatures from planktonic foraminifera. Journal of Foraminiferal Research 5, 102–113.

Bethoux, J., 1980. Mean water fluxes across sections in the Mediterranean sea, evaluated on the basis of water and salt budgets and observed salinities. Oceanologica Acta 3, 79–88.

Birks, H.J.B., Line, J.M., Juggins, S., Stevenson, A.C., terBraak, C.J.F., 1990. Diatoms and pH reconstruction. Philosophical Transactions of the Royal Society of London B 327, 263–278.

Bolli, H.M., Saunders, J.B., 1985. Oligocene to Holocene low latitude planktic foraminifera. In: Bolli, H.M., Saunders, J.B., Perch-Nielsen, K. (Eds.), Plankton Stratigraphy. Cambridge Univ. Press, Cambridge, pp. 155–262.

Brunner, Ch. A., 1979. Distribution of planktonic foraminifera in surface sediments of the Gulf of Mexico. Micropaleontology 25, 325–335.

CLIMAP, 1984. The last interglacial ocean. Quaternary Research 21, 123–224.

Comas, M.C., Zahn, R., Klaus, A., et al., 1996. Proc. ODP, Init. Repts., vol. 161. Ocean Drilling Program, College Station, TX.

Conkright, M.E., Locarnini R.A., García H.E., O'Brien T.D., Boyer T.P., Stephens C., Antonov J.I., 2002. World Ocean Atlas 2001: Objective Analyses, Data Statistics, and Figures, CD-ROM Documentation. National Oceanographic Data Center, Silver Spring, MD.

Darling, K.F., Wade, C.M., Stewart, I.A., Kroon, D., Dinglek, R., Leigh, Leigh Brown, A.J., 2000. Molecular evidence for genetic mixing of Arctic and Antarctic subpolar populations of planktonic foraminifers. Nature 405, 43–47.

Darling, K.F., Kucera, M., Pudsey, C.J., Wade, C.M., 2004. Molecular evidence links cryptic diversification in polar planktonic protists to Quaternary climate dynamics. Proceedings of the National Academy of Sciences United States of America, vol. 101, pp. 7657–7662.

de Vargas, C., Zaninetti, L., Hilbrecht, H., Pawlowski, J., 1997. Phylogeny and rates of molecular evolution of planktonic foraminifera: SSU rDNA sequences compared to the fossil record. Journal of Molecular Evolution 45, 285–294.

Dowsett, H.J., 1991. The development of a long-range foraminifer transfer function and application to Late Pleistocene North Atlantic climatic extremes. Paleoceanography 6, 259–273.

Dowsett, H.J., Poore, R.Z., 1990. A new planktic foraminifer transfer function for estimating Pliocene–Holocene paleoeceanographic conditions in the North Atlantic. Marine Micropaleontology 16, 1–23.

Dowsett, H.J., Poore, R.Z., 1999. Last interglacial Sea-Surface Temperature estimates from the California margin: improvements to the Modern Analogs Technique. United States Geological Survey Bulletin 2171 (only on the Web).

Dowsett, H.J., Robinson, M.M., 1997. Application of the Modern Analogs Technique (MAT) of Sea Surface Temperature estimation to middle Pliocene North Pacific planktonic foraminifer assemblages. Palaeontologia Electronica 1 (http://palaeo-electronica.org/1998_1/dowsett/issue1.htm).

Dowsett, H.J., Barron, J., Poore, R., 1996. Middle Pliocene sea surface temperatures: a global reconstruction. Marine Micropaleontology 27, 13–15.

Duplessy, J.-C., Labeyrie, L., Juillet-Leclerc, A., Maitre, F., Duprat, J., Sarnthein, M., 1991. Surface salinity reconstruction of the North Atlantic Ocean during the last glacial maximum. Oceanologica Acta 14, 311–324.

Gardner, J.V., Hays, J.D., 1976. Responses of sea-surface temperature and circulation to global climatic change during the past 200.000 years in the eastern equatorial Atlantic Ocean. In: Cline, R.M., Hays, J.D. (Eds.), Investigations of Late Quaternary Paleoceanography and Paleoclimatology, Mem. Geol. Soc. Am., vol. 145, pp. 221–246.

González-Donoso, J.M, Linares, D., 1998. Evaluation of some numerical techniques for determining paleotemperatures from planktonic foraminiferal assemblages. Revista Española de Paleontología 13, 107–129.

González Donoso, Serrano, F., Linares, D., 1999. Sobre la estimación de la temperatura de las aguas marinas superficiales del Plioceno a partir de un conjunto de calibración reciente. Revisita Española de Paleontología, N° Extraord. hom. Prof. Truyols, pp. 89–96.

González Donoso, Serrano, F., Linares, D., 2000. Sea surface temperature during the Quaternary at ODP Sites 976 and 975 (western Mediterranean). Palaeogeography, Palaeoclimatology, Palaeoecology 62, 17–44.

Gorshkov, S.G. (Ed.), 1978. World Ocean Atlas, vol. 2. Atlantic and Indian Oceans. Pergamon Press, Oxford, p. 305.

Hopkins, T.S., 1985. Physics of the Sea. In: Margalef, R. (Ed.), Western Mediterranean. Pergamon Press, Oxford, pp. 100–125.

Hutson, W.H., 1977. Transfer functions under no-analog conditions; experiments with Indian Ocean planktonic foraminifera. Quaternary Research 8, 355–367.

Hutson, W.H., 1980. The Agulhas Current during the Late Pleistocene, analysis of modern faunal analogs. Science 207, 64–66.

Hutson, W.H., Prell, W.L., 1980. A paleoecological transfer function, FI-2, for Indian Ocean planktonic foraminifera. Journal of Paleontology 54, 381–399.

Iaccarino, S., 1985. Mediterranean Miocene and Pliocene planktic foraminifera. In: Bolli, H.M., Saunders, J.B., Perch-Nielsen, K. (Eds.), Plankton Stratigraphy. Cambridge Univ. Press, Cambridge, pp. 283–314.

Imbrie, J., Kipp, N.G., 1971. A new micropaleontological method for quantitative paleoclimatology. Application to a late Pleistocene Caribbean core. In: Turekian, K.K. (Ed.), The Late Cenozoic glacial ages. Yale Univ. Press, New Haven, pp. 71–131.

Imbrie, J., Donk, J., Kipp, N.G., 1973. Paleoclimatic investigation of late Pleistocene Caribbean deep-sea cores. Comparison of isotopic and faunal methods. Quaternary Research 3, 10–38.

Kallel, N., Paterne, M., Duplessy, J-C., Verganud-Grazzini, C., Pujol, C., Labeyrie, L., Arnold, M., Fontugne, M., Pierre, C., 1996. Enhanced rainfall in the Mediterranean region during the last sapropel event. Oceanologica Acta 20, 697–712.

Kellogg, T.B., 1976. Late Quaternary climatic changes: evidence from deep-sea cores of Norwegian and Greenland Seas. In: Cline, R.M., Hays, J.D. (Eds.), Investigations of Late Quaternary Paleoceanography and Paleoclimatology, Mem. Geol. Soc. Am., vol. 145, pp. 77–110.

Kennett, J.P., Srinivasan, M.S., 1983. Neogene Planktonic Foraminifera: A Phylogenetic Atlas. Hutchinson Ross, Stroudsburg, PA.

Kipp, N.G., 1976. New transfer function for estimating past sea-surface conditions from sea-bed distribution of planktonic foraminiferal assemblages in the North Atlantic. In: Cline, R.M., Hays, J.D. (Eds.), Investigations of Late Quaternary Paleoceanography and Paleoclimatology, Mem. Geol. Soc. Am., vol. 145, pp. 3–41.

Klovan, J.E., Imbrie, J., 1971. An algorithm and Fortran-IV program for large scale Q-mode factor analysis and calculation of factor scores. Mathematical Geology 3, 61–77.

Kucera, M., Darling, K.F., 2002. Cryptic species of planktonic foraminifera: their effect on palaeoceanographic reconstructions. Philosophical Transactions of the Royal Society of London 360, 695–718.

Le, J., 1992. Paleotemperature estimation methods: sensitivity test on two western equatorial Pacific cores. Quaternary Science Reviews 11, 801–820.

Loubere, P., 1981. Oceanographic parameters reflected in the seabed distribution of planktonic foraminifera from the North Atlantic and Mediterranean Sea. Journal of Foraminiferal Research 11, 137–158.

Lourens, L.J., Hilgen, F.J., Gudjonsson, L., Zachariasse, W.J., 1992. Late Pliocene to early Pleistocene astronomically forced sea surface productivity and temperature variations in the Mediterranean. Marine Micropaleontology 19, 49–78.

Maslin, M.A., Shackleton, N.J., Pflaumann, U., 1995. Temperature, salinity and density changes in the Northeast Atlantic during the last 45,000 years: Heinrich events, deep water formation and climatic rebounds. Paleoceanography 10, 527–544.

Molfino, B., Kipp, N.G., Morley, J.J., 1982. Comparison of foraminiferal, coccolithophorid, and radiolarian paleotemperature equations, assemblage coherency and estimate concordancy. Quaternary Research 17, 279–313.

Molina-Cruz, A., Thiede, J., 1978. The glacial eastern boundary current along the Atlantic Eurafrican continental margin. Deep-Sea Research 25, 337–356.

Pflaumann, U., Duprat, J., Pujol, C., Labeyrie, L.D., 1996. SIMMAX: a modern analog technique to deduce Atlantic sea-surface temperatures from planktonic foraminifera in deep-sea sediments. Paleoceanography 11, 15–35.

Prell, W.L., 1985. The stability of low latitude sea-surface temperatures: an evaluation of the CLIMAP reconstruction with emphasis on the positive SST anomalies. Washington D.C. (Tech. Rep. TR025).

Pujol, C., 1980. Les foraminiferes planctoniques de l'Atlantique Nord au Quaternaire. Ecologie-Stratigraphie-Environnement. Mémoires de l'Institut de Géologie du Bassin d'Aquitaine 10, 1–254.

Serrano, F., González-Donoso, J.M., Linares, D., 1999. Biostratigraphy and paleoceanography of the Pliocene at Sites 975 (Menorca Rise) and 976 (Alboran Sea) from a quantitative analysis of the assemblages of planktonic foraminifers. In: Comas, M.C., Zahn, R., Klaus, A., et al. (Eds.), Ocean Drilling Program Leg, Scientific Results, vol. 161, pp. 185–195. Texas.

Thunell, R.C., 1978. Distribution of recent planktonic foraminifera in surface sediments of the Mediterranean Sea. Marine Micropaleontology 3, 147–173.

Thunell, R.C., 1979a. Pliocene–Pleistocene paleotemperature and paleosalinity history of the Mediterranean Sea, results from DSDP sites 125 and 132. Marine Micropaleontology 4, 173–187.

Thunell, R.C., 1979b. Climatic evolution of the Mediterranean Sea during the last 5.0 million years. Sedimentary Geology 23, 67–79.

Vergnaud-Grazzini, C., 1985. Mediterranean late Cenozoic stable isotope record: stratigraphic and paleoclimatic implications. In: Stanley, D.J., Wezel, F-C. (Eds.), Geological Evolution of the Mediterranean Basin. Springer-Verlag, New York, pp. 413–451.

Zachariasse, W.J., Zijderveld, J.D.A., Langereis, C.G., Hilgen, F.J., Verhallen, P.J.J.M., 1989. Early late Pliocene biochronology and surface water temperature variations in the Mediterranean. Marine Micropaleontology 14, 339–355.